

# Possible effect of solar activity on variation of the tree-rings of a *platycladus orientalis* at the Mausoleum of Emperor Huang

FENG Bo<sup>1,2†</sup> & HAN YanBen<sup>1</sup>

<sup>1</sup> Xi'an Institute of Posts & Telecommunications, Xi'an 710061, China;

<sup>2</sup> National Astronomical Observatories, Chinese Academy of Sciences, Beijing 100012, China;

**The variation of the tree-ring's index of a *platycladus orientalis* at the Mausoleum of Emperor Huang and of a long series of sunspots relative number during AD1470–1974 are analyzed by using the wavelet power spectrum method, and their variation characters are also discussed. It is determined that the tree-ring's variation has cycles of approximate 2–7, 11, 93 and 150 a. Two data series are used for analyzing sunspot relative number (SSN) variation. First, the analysis of the annual average SSN during AD1700–1974 proved that variation cycles are about 11, 50, and 93 a; then, the data during AD1465–1975 obtained from the decadal average SSN train over 7000 a reconstructed on the geomagnetic data is analyzed and its variation cycles are about 50, 90, and 160 a. Besides the tree-rings cycle of 2–7 a is commonly considered to be related to ENSO, while 11 a cycle is related to solar Schwabe cycle; in addition, it is possible that the cycles of 90 and 150 a are likely to be related to solar Gleissberg cycle and Suess cycle. The correlations between them are possibly due to the effect of solar activity on the climate and additionally on the tree's growth.**

tree-ring, solar activity, climate change, wavelet spectrum

The effect of solar activity on the global climate is an important scientific matter of the cross-subject as well as a scientific fundament. Various high-tech measurement methods and non-linearity theory are adopted by the scholars in the world for studying the cross-subject integral activity. Our target is to further recognize the mechanism of global climate change, and to evaluate the effect of the astronomical element and the humanity activity on the global change. Due to the lacking of historic climate record and solar activity, the tree-ring's data is regarded as one of the most important data for studying the Past Global Changes (PAGES), because it has some advantages such as the precise-yearing, strong-continuity, high-resolution, and duplicates are easily obtained. Some scientists consider that the records of numerous tree-rings responding to variations of various climate parameters on most part of the earth to be supe-

rior to any other substitute index of which the measurement period can be scaled as a year. Therefore, the studies of the tree-ring's and climatic change and solar activity have become popular recently. In the beginning of the 20th century, Douglas<sup>[1]</sup> connected the annual tree-ring's width of the cypress at Arizona during 1660–1720 with solar Maunder Minimum.

In China, since the 1930's the analysis of the tree-ring and the research of the previous climate by using the tree-ring's width variations have been developed. Especially during the 1970–1980's, with the advance of the research of the climatic change, tree-ring's climatology has been developed rapidly. Wu et al.<sup>[2]</sup> sampled the

Received October 16, 2007; accepted April 30, 2008  
doi: 10.1007/s11433-009-0048-7

†Corresponding author (email: fengbor@sina.com)

Supported by the National Natural Science Foundation of China (Grant No. 19373017)

tree-rings on a large scope at Huanghe valley, Qinling mountains, and the eastern Tianshan mountains for many times and carried out a series of researches of the tree-ring's and climatic change. Shaanxi Province Meteorological Bureau sampled the tree-rings of the cypress at the Mausoleum of Emperor Huang (MEH) in 1975. Li et al.<sup>[3]</sup> applied these data to study the climate change over 500 a at Shaanxi. In 1992, Peng et al.<sup>[4]</sup> applied the Maximum-Entropy Method to analyze the cyclical variation of the tree-rings of the cypress at the MEH and SSN, and indicate that some tree-ring's cycles is related to solar activity. In 1995 Hong et al.<sup>[5]</sup> researched the relationship between the variation of the oxygen-isotope of the peat plants over 5000 a at Jinchuan and solar activity. Some scholars considered that solar activity can influence the global environment in many aspects<sup>[6]</sup>. In 2004, Zhong et al.<sup>[7]</sup> studied solar activity and the climate fluctuations over 4000 a at Tarim Basin. In 2007, Sang et al.<sup>[8]</sup> analyzed the tree-ring's width of the dragon spruce at Tianshan mountains and the gradient meteorological parameter.

Solanki et al.<sup>[9]</sup> used  $^{14}\text{C}$  radioactivity measurement technology to reconstruct the SSN data over 11400 a on the tree-rings. Eddy, a well-known solar-terrestrial physicist, considered that although many studies have been done, the clear correlation between the solar and the climatic change has yet not been constructed. Most of the correlation-ship are dubious and opposed as they almost all may be shaken by the strict statistically examination or be defeated by the different data examination. The convincible physics mechanism has not yet produced when the variation of the cycle of 22 a achieved by using the tree-ring's width over 370 a at the western of US was recommended. And the drought period reflected by the tree-rings is subtle. It is a variable when the tree-rings are at different area in the extensive district. He emphasized the processing of data required strict statistical examination, and must follow objective standards of data analysis, and thus some chaos arising from the researches can be avoided.

Up to now, the studies of the relationship between the Sun and climate have been suspected, so a large number of data on the different time scale and on the various regions for further studying is required for this problem. Therefore we make a strict examination and use a new non-linearity analysis way, wavelet analysis, for studying this problem. An important methodology to study the

correlation between the climatic change and the solar activity is to explore if there is some similar cyclical change<sup>[11]</sup>. Thus we apply the wavelet power spectrum analysis method to study the SSN and cyclical changes of the tree-rings of the cypress at MEH, in order to provide the further evidences for studying the relationship between the climatic change and solar activity.

## 1 The data and analysis method

### 1.1 The tree ring data

The tree-ring's width's data is adopted from ref. [3]. The sampling series is of the combined tree-ring's indexes of an oriental arborvitae at MEH (wherein the elevation of 980 m, the slope of  $40^\circ$  with facing to North-west) at Huangling county ( $35^\circ 31' \text{N}$ ,  $109^\circ 12' \text{E}$ ), and of an oriental arborvitae at the mausoleum of Liu (wherein the elevation of 930 m, the slope of  $15^\circ$  with facing to South.) at Liyuan, of 7 km distance from Huangling county town. The tree-ring's sample is taken from the upper of the wood, the cutting-point is of 30 cm above the earth surface. The length of the series is of 505 (AD1470—1974), shown in Figure 1. By calculating, of the tree-ring's series the autocorrelation coefficient is achieved as high as of 0.9 and its standard deviation is of 0.38 mm.

### 1.2 The data of solar activity

SSN has always be considered as a main parameter of the intensity of solar activity. Its data since AD1700 are taken from ref. [12]. Because the time range of this series is only of 300 a, it is difficult to examine the cycles longer than 100 a. In order to analyze longer cycles, the decadal-smoothing-mean-value series of SSN during BC4955—AD1995 founded by Usoskin et al.<sup>[13]</sup> is applied. For being wholly identical with the starting point of the tree-ring, the data during AD1465—1975 from the series above is applied.

### 1.3 Wavelet analysis method

For measuring the abrupt point of the series, Mallat's algorithm for discrete wavelet is usually applied. As for a discrete wavelet evaluation, the date-base is of 2, and the analysis using the wavelet power spectrum of this series can't achieve some specified cycles. Therefore we make the analysis by using a consecutive wavelet, which is usually applied to problem analysis and theoretic research, and to more thoroughly understand the fundamental character of the wavelet and the analytical signal.

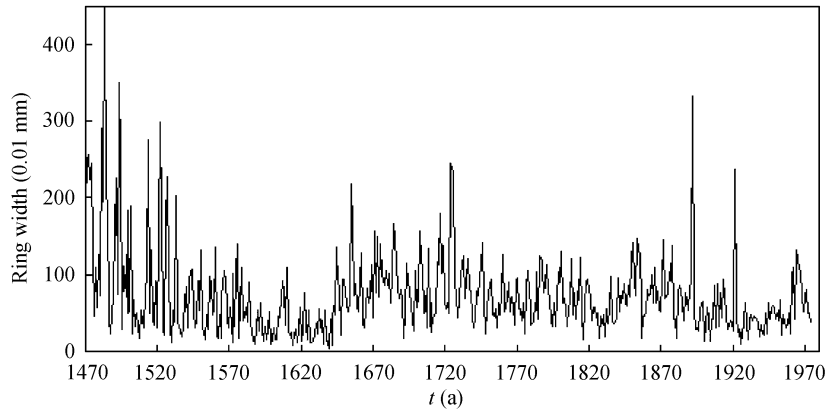


**Figure 1** The tree-ring's width of a platycladus orientalis at the mausoleum of Emperor Huang.

A continuous wavelet transformation of a series of a discrete time series is defined as the convolution integral of the time series of  $x(t)$  and a mother wavelet function  $h(\eta)$ :

$$W(a, b) = \frac{1}{\sqrt{a}} \int_{-\infty}^{\infty} x(t) h(\eta) dt, \quad (1)$$

where  $h = (t - b)/a$ ,  $a$  is the dilatation parameter and  $b$  is the translation parameter.

A mother wavelet function  $h(\eta)$  is defined as

$$h(\eta) = |a|^{\frac{1}{2}} h\left(\frac{t-b}{a}\right). \quad (2)$$

The Morlet wavelet, which is usually applied in geophysics and astronomy, is selected as the mother wavelet in this work. Han et al.<sup>[15]</sup> and Song et al.<sup>[16]</sup> respectively applied the Morlet wavelet to analyze the cyclical changes of SSN and photosphere magnetic flux. It is the product of the function of wave in a plane and the Gaussian function:

$$h\left(\frac{t-b}{a}\right) = \pi^{-1} \exp\left(i\omega_0 \frac{t-b}{a}\right) \exp\left[-\frac{1}{2}\left(\frac{t-b}{a}\right)^2\right]. \quad (3)$$

Although its local time-frequency performance is quite well, in the strict sense, it satisfies with neither the finite supported arm nor the admissibility condition. However, in practical situation, if we provide  $\omega_0 \geq 5$ , the conditions could be approximately satisfied. So we choose  $\omega_0 = 6$ , where  $\omega_0$  is a non-dimensional frequency. The Morlet wavelet function is complex, meaning the wavelet transformed is also complex and can be divided into a real and an imaginary part or an amplitude and a phase spectrum. The square of the amplitude of the wavelet transformed,  $|W(a, b)|^2$ , is called as the wavelet power spectrum. On the basis of the discussion above, we will evaluate the tree-ring's wavelet power

spectrum.

Beside the choice of the mother wavelet, the definition of the set of dilatation parameter  $a$  is necessary to satisfy

$$a_j = a_0 2^{j\delta_j}, \quad j=0, 1, 2, 3, \dots, J, \quad (4)$$

where  $a_0$  is the smallest and  $a_J$  is the largest dilatation parameter.  $J$  is chosen as

$$J = \delta_j^{-1} \log_2(N\delta t / a_0), \quad (5)$$

where  $a_0$  is chosen in such a way that the corresponding Fourier period is  $2\delta t$ , and  $\delta_j = 0.125$  is a parameter which affects the resolution and leads to a smooth picture of the wavelet power spectrum. The wavelet power spectrum  $|W(\lambda, t)|^2$  is depended on the Fourier period  $\lambda$  and the time  $t$ , whereby the translation parameter  $b$  corresponds to the time step  $\delta t$  of the time series. The relation between the dilatation parameter  $a$  and the equivalent Fourier period  $\lambda$  can be analytically deduced for the Morlet wavelet by applying a cosine oscillation with known Fourier period in eq. (1). The dilatation parameter  $a$ , which reaches the maximum in the wavelet power spectrum is related to the Fourier period  $\lambda$ . For the Morlet wavelet the relation is

$$\lambda = \frac{4\pi a}{\omega_0 + \sqrt{2 + \omega_0}}, \quad (6)$$

where we found  $\omega_0 = 6$ ,  $\lambda = 1.03a$ , and thus, the dilatation parameter  $a$  is similar to the Fourier period of the Morlet wavelet.

For the algorithm, the time series has to be filled with zeros at the beginning and the end, so that the length of this new time series is a power of 2.

For interpreting the maximum of the wavelet power spectrum, the statistical significance test is applied. Al-

though some maximums can be found from the wavelet power spectrum diagram, the false maximums will appear due to the effect of the noise, corresponding to the true periodic component of the signals, which can't be determined, and thus the statistical examination is required for the determination. Set the noise in the signal as a complete Gaussian distribution with a variance of  $\sigma^2$ , and the wavelet noise spectrum  $P_{\text{noise}}(a,b)$  is as a  $\chi^2$  distribution. In this case the Morlet wavelet is complex, and its distribution has two degrees of freedom, i.e.,

$$P_{\text{noise}} \Rightarrow \frac{1}{2} \sigma^2 \chi^2. \quad (7)$$

The significant level can be evaluated by using the eq. (7). The signal is usually separated with 95% the significance level from the background noise. It can be explained as that the maximums achieved from the wavelet power spectrum diagram are true, and are not caused by the noise. Thus we will note 95% the significance level for the wavelet spectrum in the next section.

As the raw data's number is finite, and the convolution is applied for the wavelet calculation, hence it leads to the abrupt change on the edge, i.e., the edge effect. To avoid this effect, the mirror-reflection and then the periodic extension have to be applied before the data procession for all of the data series. Hence the abrupt change on the edge can be avoided.

## 2 Wavelet analysis and results

### 2.1 The tree-ring's wavelet spectrum

We analyze the tree-rings of the oriental arborvitae at the MEH by using the wavelet analysis, and achieve its

wavelet power spectrum as shown in Figure 2. The tree-ring's normalized standard variance (This choice is for conveniently calculating the wavelet.) is shown as Figure 2(a), the wavelet power spectrum is shown as Figure 2(b). Its horizontal axis represents the year of the Christian era and the vertical as the period (unit: a). The closed line in the Figure 2(b) displays that wherein the 95% significance level is exceeded. Figure 2(c) shows the global wavelet power spectrum of the tree-ring's index, and the dotted line shows the 95% significance level. That of the cycles of 2–7, 11, 150, and 260 a exceeds the 95% significance tests.

### 2.2 Wavelet spectrum of sunspot number

SSN in ref. [11] has 3 clear cycles of 11, 50, and 93 a. The 11 and 93 a pass the 95% significance test. Although the 50 a is relatively clear, it has not yet reached the 95% significance level (Figure 3). The cycle of 11 a is similar to the well-known Schwabe cycle, the 93 a approaches to the Gleissberg cycle, and the 50 a is achieved by using the wavelet analysis. Le et al.<sup>[17]</sup> used the wavelet analysis and achieved the cycles of 11, 53, 101 a. In the recent years, Li et al.<sup>[18,19]</sup> made the wavelet analysis for the monthly-mean-values of SSN, of sunspot area and of sunspot element area, and deeply researched the edge effect of the wavelet analysis.

For analyzing the cycle which is equal to or larger than 100 a, the data during AD1465–AD1975 in ref. [12] are applied for analysis. Four relatively clear cycles 50, 90, 160 and 270 a are achieved. But except for 160 a, all other cycles cannot pass the 95% confidence test (see Figure 4).

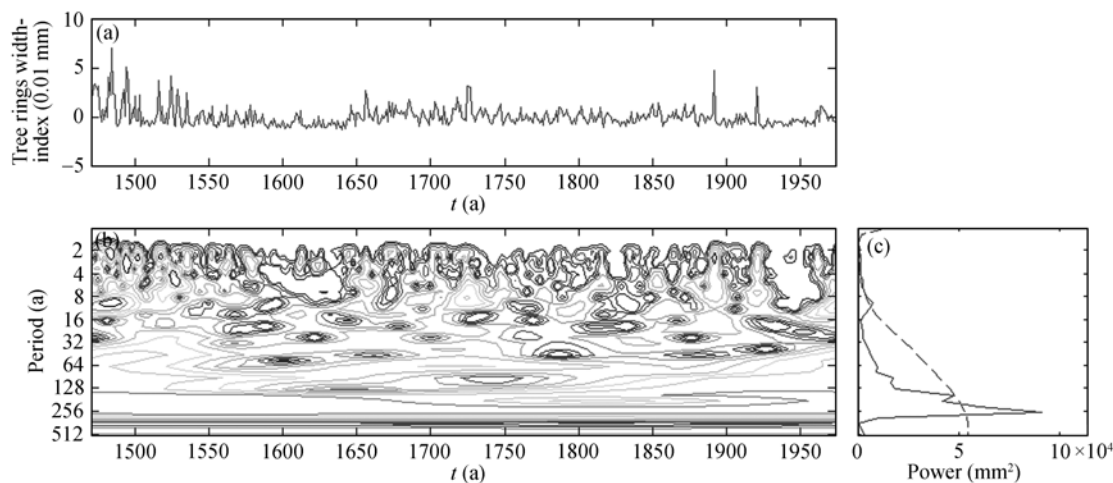


**Figure 2** The wavelet power spectra of the tree-rings. (a) Tree rings normalize by standard deviation; (b) tree rings wavelet power spectrum; (c) global wavelet spectrum.

### 3 Discussion and conclusion

Some scholars pointed out that in general the tree-ring width's variation mainly reflects the temperature variation in the cold and humid mountains, and reflects the humidity or rainfall variation in the arid or semiarid and warm area<sup>[20]</sup>. Huangling is situated on the southern of the Loess's Plateau which is a warm and semiarid area, and hence the tree-ring width's variation of the *Platycladus orientalis* at the MEH mainly reflects the annual rainfall variation on this area. Li et al.<sup>[3]</sup> once thoroughly analyzed the relationship between the tree-rings and the climate in Shaanxi and northern Shaanxi. They achieved results that indicate the range with the higher value of the tree-ring's width corresponds to the humider time range in the humidity series at Yan'an area, and corresponds mainly to the colder time range of the country-wide temperature variation, additionally the range with the lower value of the tree-ring's width corresponds to the arider time range in the humidity series at Yan'an area, and corresponds mainly to the warmer time range of the country-wide temperature variation. They also found that the correlation coefficient between the tree-rings and the rainfall on the neighbor area of Luochuan and Yan'an during various time ranges is respectively 0.33 and 0.38, and correlation coefficient of the variation between the tree-rings and the Xi'an temperature is about -0.34. All of these consequences pass the 95% significance test. By applying Mallat algorithm to the discrete wavelet method we detected the abrupt changes of the tree-ring's, which is at years such as 1580, 1644, 1724, 1892 and 1921. The series of the tree-rings is divided into 6 time ranges on the basis of the wavelet amplitude (see Figure 5), such as AD1470—1580 (higher), AD1581—1644 (lower), AD1645—1724 (higher), AD1725—1891 (lower), AD1892—1921 (higher), and AD1922—1974 (lower).

Three historical critical droughts respectively happened in 3 lower-value's time ranges. In the north of Shaanxi, a critical drought lasted for 6 a during AD1636—1641. In the middle of Shaanxi, a critical drought lasted for 7 a during AD1635—1641. The response of the tree-rings is very clear. Two minimum tree-rings respectively happened in 1639 and 1641, which is very clear during this time range. During AD1874—1878, a critical drought lasted for 5 a, and a drought happened in 1929 again. In fact, the drought northern Shaanxi hap-

pened earlier and lasted longer. All of the tree-rings during 1923-1932 are narrower. Especially the third minimum value of tree-ring series happened in 1925. According to the historic record, a torrential rain lasted for 17 days during Sept. 20—Oct. 6, 1662. The tree-ring's width at this year is several times wider than the adjacent years. It shows that the tree-ring's indexes over 500 a at the MEH can reflect the change rule of the climate such as humidity and temperature in Shaanxi.

In order to study the relationship between solar activity and the tree-ring index, the cross-correlation between SSN and the tree-ring index has been analyzed by using the convolution method and the correlation curve for all data is shown in Figure 6(a). As the data is so concentrated, we zoom a part of the curve in Figure 6(b). From Figure 6(b) we can find that the correlation coefficient is the largest while the tree-ring lags 2 a behind SSN. It shows that the tree-ring variation is controlled by solar activity.

About the common cyclical variation character of solar activity and the tree-rings, we can see that SSN and the tree-rings of the oriental arborvitae at the MEH have several relatively common cycles in Figures 2—4. For convenience of the analysis, we will respectively analyze these cycles in Figure 7. The tree-ring's cycle of 2—7 a is generally considered as the variation related to ENSO (El Nino Southern Oscillation). Here we will not discuss it any more.

Although that the tree-rings and SSN have been made a periodic extended treatment to reduce the edge effect, the longer cycles of about 260 a for the tree-ring's and about 270 a for SSN are probably to a certain extent influenced by the edge effect, and therefore their precision is dubious. It is inferred inconvincible that there is a cycle of about 200 a. Thus we will only analyze the common cycle of 11, 90, and 160 a. Ogurtsov et al.<sup>[23]</sup> analyzed the long-term variation of solar activity and achieved that it has the cycles of 50—80, 90—140, and 160—260 a. They considered the first two are belonged to the Gleissberg cycle, of which the time scale is about 100 a, and the last is to Suess cycle.

Of the Schwabe cycle of SSN, the wavelet amplitude during 1700—1974 has very large fluctuations. Its lowest appears during 1800—1810 and largest appears in about 1960. The variation of the tree-ring's amplitude of 11 a is relatively large. It is opposite to the variation of the tree-rings during the greater part of the time

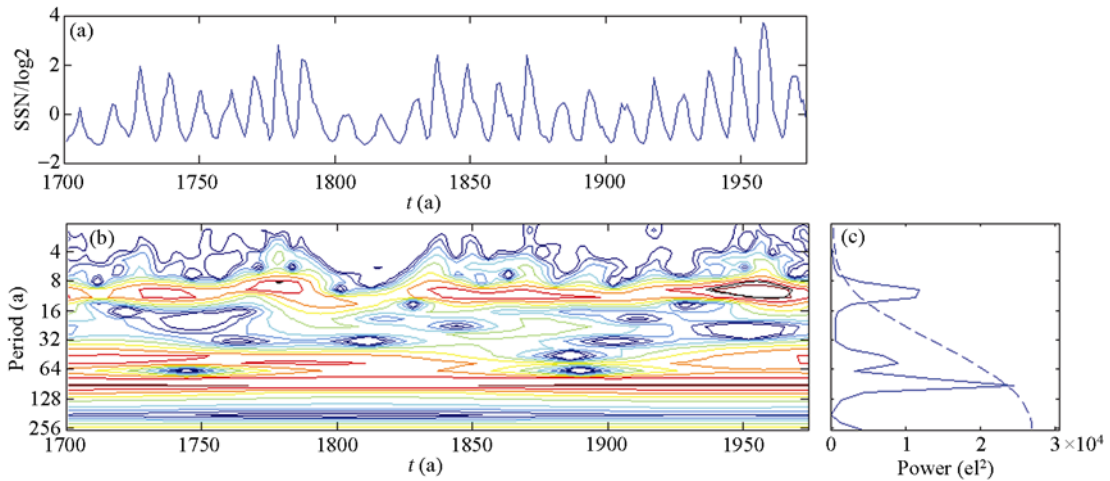


**Figure 3** The wavelet powerspectrum of the sunspot number (1700–1974). (a) SSN normalized by standard deviation; (b) SSN wavelet power spectrum; (c) global wavelet spectrum.

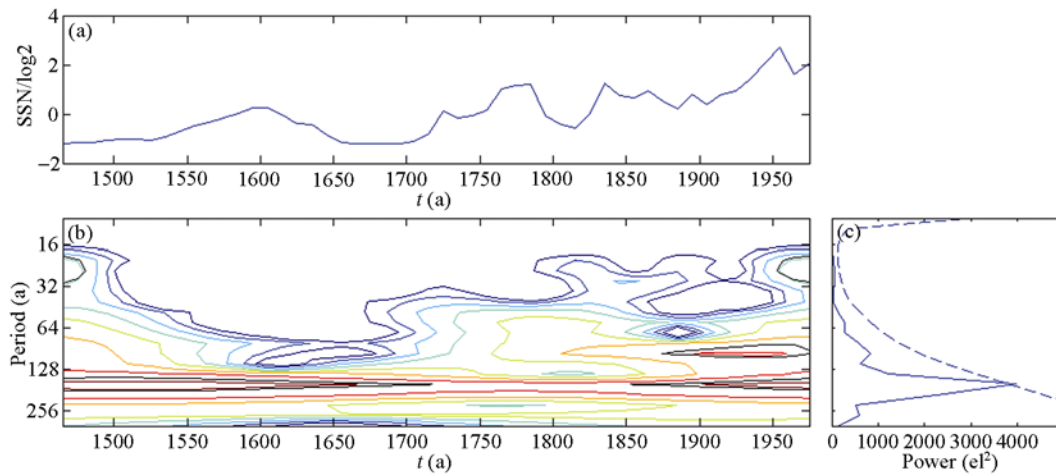


**Figure 4** The spectrum of the decadal-mean-values of sunspot (1464–1975). (a) SSN normalized by standard deviation in the AD1465–1995; (b) SSN wavelet power spectrum; (c) global wavelet spectrum.

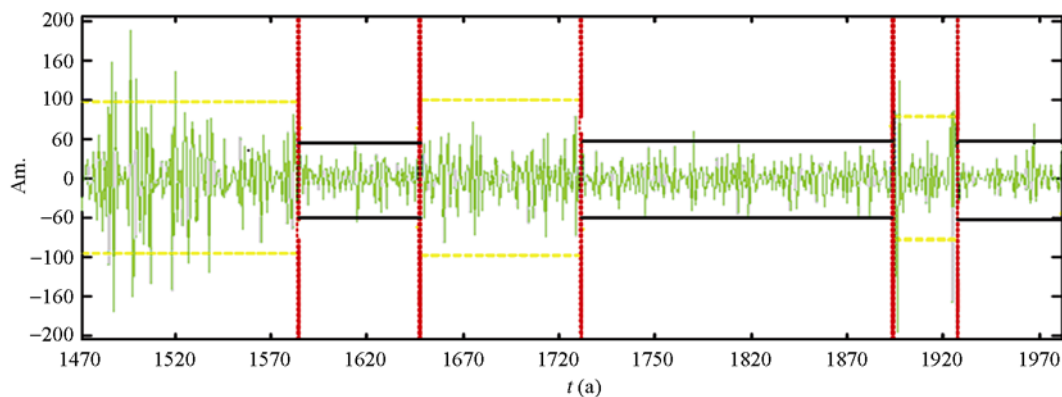


**Figure 5** 6 time ranges divided on the tree-ring’s wavelet amplitude (Am.).

range. Except for two time ranges round AD1720 and AD1780, the SSN’s amplitudes are larger than the tree-ring’s.

The wavelet amplitude of the Gleissberg cycle is

slightly smaller than the Schwabe cycle’s. However both the tree-ring’s and SSN appear a basically similar variation “W” pattern. Two lowest values appear in 1760 and 1900. Before 1850, SSN’s amplitude is larger than the

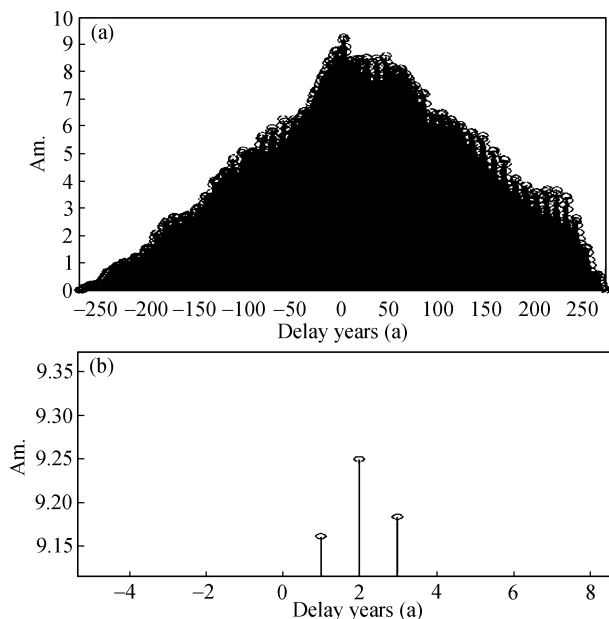


**Figure 6** Correlation between the sunspot number and the tree-ring's index.

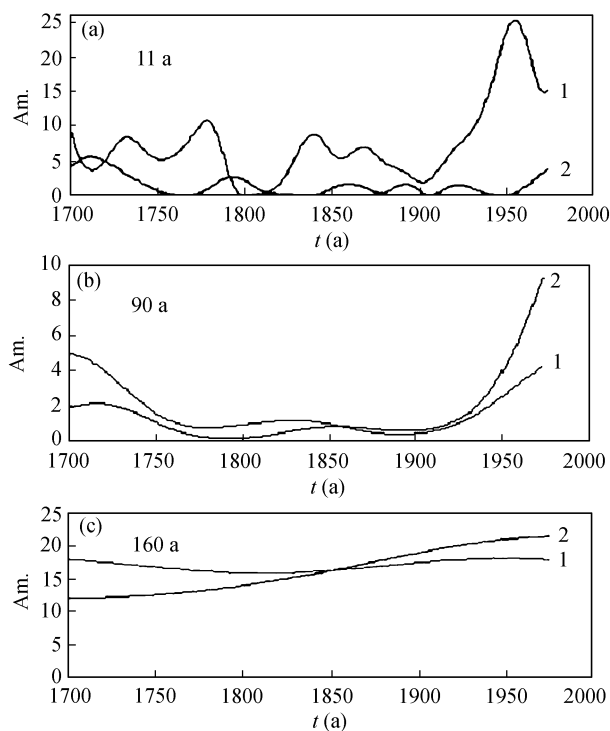


**Figure 7** Variation of the main cycles of (1) the sunspot number and (2) the tree-ring.

tree-ring's, but after 1850, it is opposite.

The wavelet amplitude of the Suess cycle shows relatively large. However both SSN's and the tree-ring's fluctuations are relatively low. They appear a variation shape of quasi-“W”. The difference is that before 1850, the SSN's amplitude is larger than the tree-ring's, but since 1850, the opposite variation appears.

Moreover, we can see that there are two apparent large-size tree-ring's variations. The tree-ring's higher-value range (AD1470–1580) is respectively in the solar Sporer's Minimum (AD1420–1570). The tree-ring's higher-value range (AD1645–1724) is respectively in the solar Maunder's Minimum (AD1420–1570). It shows that the relation between the tree-rings of the cypress at the MEH and the climatic variation and solar activity is consistent with this relation in other areas all over the world.

In short, the tree-ring's wavelet cycles are related to the well-known solar Gleissberg cycle and Suess cycle, as well as the most prominent Schwabe cycle. It should be noted that on each of the first two, there is a break point at 1850. It probably reflects that since 1850, the increase of humanity activity has effect on the climate.

For the solar-climatic problem related to the studying for the mechanism of the phenomena above, some well-known solar-terrestrial physicists from all over the world such as Tu<sup>[24]</sup>, Zhuang<sup>[25]</sup>, Lin<sup>[26]</sup>, Shi<sup>[27]</sup>, and Frieman et al.<sup>[28]</sup> separately made some discussions in their treatises. But up to now, this problem has not been solved. We consider that only by using the sunspot index (including SSN, sunspot mass, and sunspot area) is not enough for the research. Its extensive application is due to its longer measurement data. Because the sunspot indexes can only reflect the sunspot structural activity and they only have a qualitative performance, they are difficultly related to the mechanical and the energetical processes in the physical research. To find the effect of solar activity on the earth environment, three main factors have to be considered.

The first one is the solar electromagnetic radiation. It contains both solar constant's variation and solar ultraviolet radiation. Many climatic parameters have the variation of the cycle of 11 a. The most clear is the solar constant and of the troposphere temperature<sup>[29]</sup>. It's achieved by the calculation that the troposphere temperature increases roughly 0.4 K while solar constant increases 1 W/m<sup>2</sup>. During the Schwabe cycle, the total solar radiation variability is only of 0.1%. The variability is too small to interpret the troposphere temperature variation. The ultraviolet radiation should be considered. The contribution of the radiation at this waveband to solar constant is very small, but it controls the ozone in the stratosphere and the photochemistry in the middle layer. The ozone magnifies the responsibility the strato-

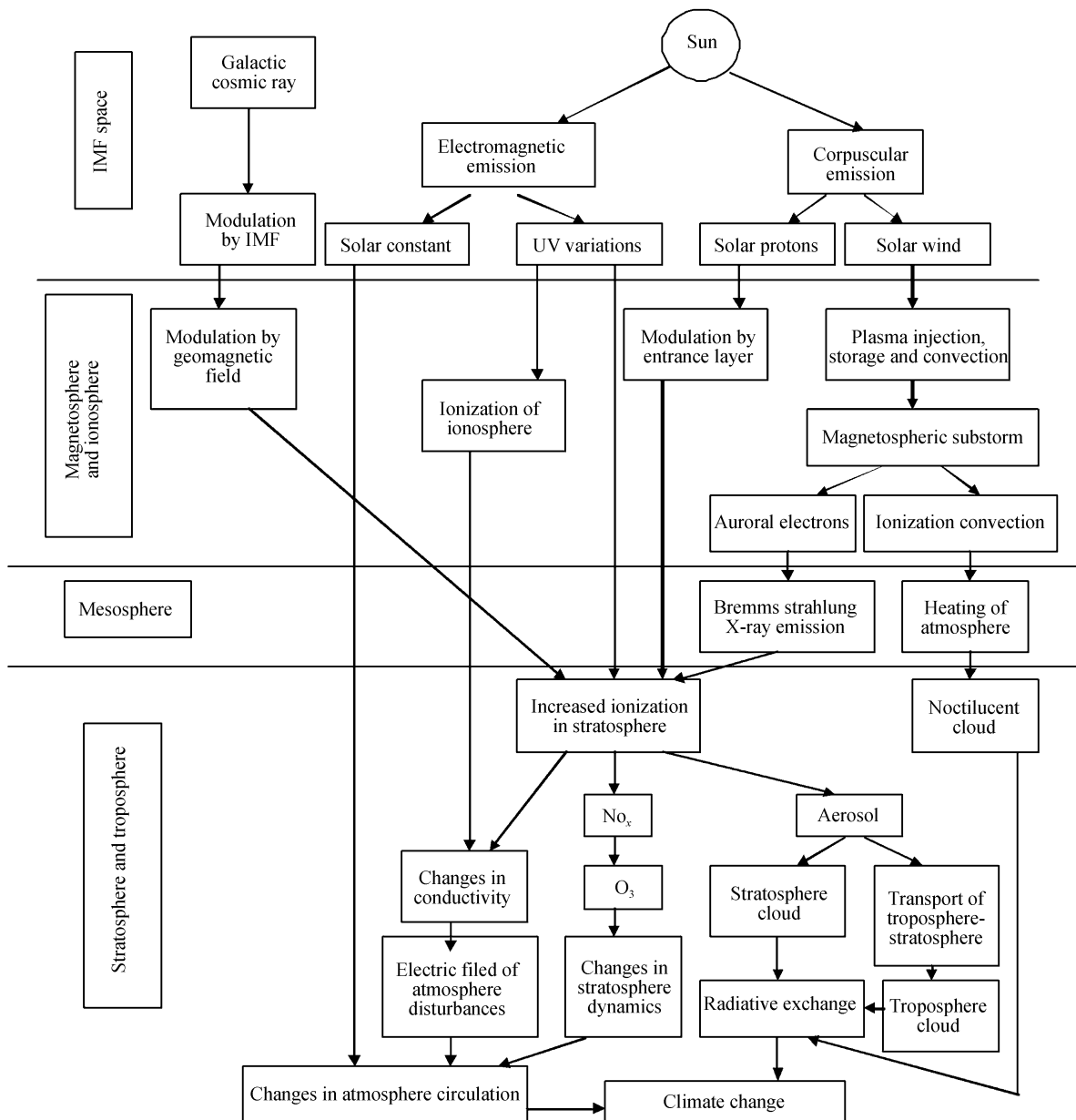


Figure 8 The physical mechanism of the climatic variation related to solar activity.

sphere to solar activity. Although the solar constant variation during a time range of 11 a is relatively small, the solar constant variation during a larger time range such as the Gleisberg cycle will probably become even larger, and the effect on the climate is even more important. The research of the quasi-sun star shows that since the Maunder Minimum, the solar constant variability has ever been as high as 0.6<sup>[30]</sup>. It drives the deep development of the study of the effect of solar variation on the climate.

The second one is the effect of solar wind. The history of the direct measurement on solar wind in the outer

space is only 30 a more. We can only achieve its variation characters corresponding with the solar variation of the cycle of 11 a. On the year in which SSN is lower, the solar wind's density is relatively large and its speed is relatively small, but on the year in which SSN is higher, the opposite variation appears. Boberg<sup>[32]</sup> analyzed the concerned parameters of solar wind and of the lower atmosphere and found that the solar wind electric field modulates NAO (North Atlantic Oscillation) and offered the evidence of the direct effect of solar wind on the lower atmosphere.

Last, it is the effect of the galactic cosmic ray. Al-

though the galactic cosmic ray is not directly related to the Sun, but it has to be modulated by the solar wind magnetic field, and its variation is opposite to the variation of the solar cycle of 11 a. Pudovkin et al.<sup>[33]</sup> found that the cloudiness over the measurement area apparently decreases while the solar activity increases as the cosmic ray flux decreases. In the later, Svensmark et al.<sup>[34]</sup> found that the cloudiness over the measurement area apparently decreases while the galactic cosmic ray flux decreases. During the solar cycle of 11 a, their variability is roughly of 3%–4% and the correlation coefficient between them is as high as of 0.95. It shows

that there is a direct link between the galactic cosmic ray flux incidence on the Earth and the cloudiness.

In summary, on the basis of physical mechanism block-diagram of the solar activity and the climatic variation offered by van Geel et al.<sup>[35]</sup>, combining with a block-diagram of the solar-terrestrial physical mechanism ever offered by Feng<sup>[36]</sup>, a new detail block-diagram of the mechanism of climatic variation related to solar activity is offered here for deeply inquiring into this problem (see Figure 8).

*The authors would like to thank Dr. Korte for the SSN series over 7000 years reconstructed by themselves.*

- 1 Douglas A E. Climatic cycles and tree growth: A study of cycles. Washington: Carnegie Institute of Washington Publications, 1936, 3. 298
- 2 Wu X D, Shao X M. Status of dendroclimatological study and its prospects in China. *Adv Earth Sci*, 1993, 8(6): 31–35
- 3 Li Z Y, Li L, Wang X Q. The climatic change during the recent 500 years in Shaanxi and the ancient Cypress at the Mausoleum of Emperor Huang. In: Zou S J, ed. *The Climatic Research*. Beijing: China Meteorological Press, 1989. 90–96
- 4 Peng X M, Feng B. The periodic analyses of the Huang Ling Cypress rings and solar activity. Shaanxi: Publications of Shaanxi Observatory, 1992, 15(2): 189–192
- 5 Hong Y T, Liu D S, Jiang H B, et al. Evidence for solar forcing of climate variation from  $\delta^{18}\text{O}$  of peat cellulose. *Sci China Ser D-Earth Sci*, 2000, 43(2): 217–224
- 6 Wang J L, Sun J L. Solar activities and their effects on terrestrial environments. *Quatern Sci*, 2002, 22(6): 511–521
- 7 Zhong W, Wang L G, Tyip T, et al. Possible solar forcing of climate variability in the past 4000 years inferred from a proxy record at the southern margin of Tarim Basin. *Chin Sci Bull*, 2004, 49, 11: 6
- 8 Sang W G, Wang Y X, Su H X, et al. Response of tree-ring width to rainfall gradient along the Tianshan Mountains of northwestern China. *Chin Sci Bull*, 2007, 52(21): 2954–2962
- 9 Solanki S K, Usoskin I G, Kromer B, et al. Unusual activity of the Sun during recent decades compared to the previous 11,000 years. *Nature*, 2004, 431(7021): 1084–1087
- 10 Eddy J A. *Weather and Climate Responses to Solar Variations*. Boulder: Colo Assoc Univ Press, 1983
- 11 Stuiver M, Braziunas T F, Becker B, et al. Climatic, solar, oceanic, and geomagnetic influences on late glacial and Holocene atmospheric  $^{14}\text{C}/^{12}\text{C}$  change. *Quat Res*, 1991, 35: 1–24
- 12 Mckinnon J A. Sunspot Numbers, WCD-A, Report UAG-95, 1989
- 13 Usoskin I G, Solanki S K, Korte M. Solar activity reconstructed over the last 7000 years: The influence of geomagnetic field changes. *Geophys Res Lett*, 2006, 33(8): L08103
- 14 Torrence C, Compo G. A practical guide to wavelet analysis. *Bull Amer Meteor Soc*, 1998, 79: 61–78
- 15 Han Y B, Han Y G. *Chin Sci Bull*, 2002, 47(7): 609–612
- 16 Song W B, Wang J X. Periodicities in photospheric magnetic flux. *Sci China Ser G-Phys Mech Astron*, 2006, 49(2): 246–256
- 17 Le G M, Wang J L. Wavelet analysis of several important periodic properties in the relative sunspot numbers. *Chin J Astron Astrophys*, 2003, 3(5): 391–394
- 18 Li K J, Li Q X, Su T W, et al. The periodicity of high-latitude solar activity. *Solar Phys*, 2006, 239: 493–501
- 19 Li K J, Li Q X, Su T W, et al. The schwabe and gleissberg periods in the wolf sunspot numbers and the group sunspot numbers. *Solar Phys*, 2005, 229: 181–198
- 20 Huang C C. *The Variation of Environment*. Beijing: Science Press, 1998. 28–29
- 21 Feng B, Ding H L. The Relation Between the Droughts in the Shaanxi Province and the Solar Activity. Shaanxi: Publications of Shaanxi Observatory, 1995, 18(1): 26–31
- 22 Xu H S. Some disaster at most in Chnia. *J Catastrophol*, 1986, 1(1): 35–40
- 23 Ogurtsov M G, Nagovitsyn Yu A, Kocharov G E, et al. Long-period cycles of the sun's activity recorded in direct solar data and proxies. *Solar Phys*, 2002, 211(1-2): 371–394
- 24 Tu C Y. *Solar-Terrestrial Space Physics (2)*. Beijing: Science Press, 1988. 339–343
- 25 Zhuang H C. *Space Electricity*. Beijing: Science Press, 1995. 703–706
- 26 Lin Y Z. *Introduction to Solar Physics*. Beijing: Science Press, 2000. 554–560
- 27 Shi G Y. *Atmosphere Radiation*. Beijing: Science Press, 2007. 292–302
- 28 Frieman E A. *Solar Influences on Global Change*. Washington: National Academy Press, 1994
- 29 Christiansen F, Haigh J D, Lundstedt H. Influence of solar activity cycles on earth's climate, ESA CR. No. 18453, 2007: 4–8
- 30 Zhang Q, Soon W H, Baliunas S L, et al. A method of determining possible brightness variations of the Sun in past centuries from observations of solar type stars. *Astrophys J*, 1994, 427: L111–L114
- 31 Richardson J D, Kasper J C. Solar cycle variations of solar wind dynamics and structures. *J Atmos Sol-Terr Phys*, 2008 (70): 219–225
- 32 Boberg F, Lundstedt H. Solar wind variations related to fluctuations of the North Atlantic Oscillation. *Geophys Res Lett*, 2002, 29(15): 13–14
- 33 Pudovkin M, Veretenenko S. Cloudiness decrease associated with Forbush decrease of galactic cosmic rays. *J Atmos Sol-Terr Phys*, 1995, 57: 1349–1355
- 34 Svensmark H, Friis Christensen E. Variation of cosmic ray flux and global cloud coverage—a missing link in solar climate relationships. *J Atmos Sol-Terr Phys*, 1997, 59: 1225–1232
- 35 van Geel B, Raspopov O M, Renssen H, et al. The role of solar forcing upon climate change. *Quat Sci Rev*, 1999, 18(2): 331–338
- 36 Feng B. Solar flare and sudden change of Earth's rotation. *Chin Astron Astrophys*, 1991, 15(3): 329–335